Imaging of Electric and Magnetic Near Field

HORÁK, M.; KŘÁPEK, V.; ŠIKOLA, T.

GIT Imaging&Microscopy

vol. 3, iss. 1, pp. 31-33

ISSN (Online): 1439-4243

DOI: http://dx.doi.org/10.1002/was.000400059

preprint

Imaging of Electric and Magnetic Near Fields

Electron Energy Loss Spectroscopy in Plasmonics

Michal Horák, Vlastimil Křápek, Tomáš Šikola

Central European Institute of Technology and Institute of Physical Engineering, Brno University of Technology, Brno, Czech Republic

Localized surface plasmon resonances are self-sustained collective oscillations of free electrons in metallic nanostructures. We have demonstrated the possibility to map their electric and magnetic near field by electron energy loss spectroscopy utilizing Babinet's principle. Further, we have indicated quantitative limits of our approach due to limited validity of Babinet's principle and discussed the influence of the experimental parameters to the signal-to-background ratio.

Interaction of the electromagnetic field and free electron gas at the metal-dielectric interfaces gives rise to hybrid light-matter states called surface plasmon polaritons (SPP). Their generation and propagation is studied by a branch of nanophotonics called plasmonics. Spatially restricted interfaces, e.g. in metallic nanoparticles (so-called plasmonic antennas), support standing SPP waves – localized surface plasmon resonances (LSPR), see Figure 1. A characteristic feature of LSPR is a strong enhancement of the electromagnetic field in the surrounding dielectric together with its spatial confinement on the subwavelength scale in the vicinity of plasmonic antennas, which can be utilized in a wide range of applications including spectroscopy and sensing, energy harvesting, and medicine. Significance of LSPR is further increased by easy tunability of their spectral characteristics via engineering the size, shape, or dielectric environment of nanoparticles. Plasmonic antennas are often fabricated by electron or ion beam lithography [1].

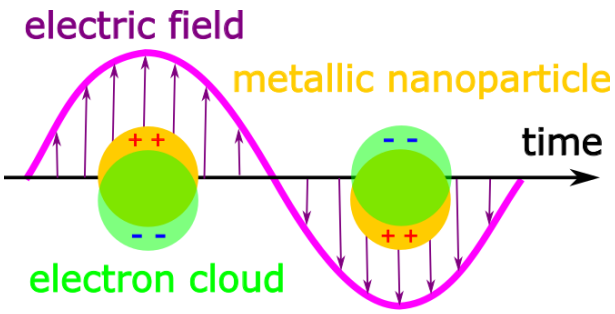

Figure 1: Free electrons in a metallic nanosphere are collectively excited by an external electric field and form a quasiparticle called the localized surface plasmon.

Mapping of LSPR modes with high spatial and energy resolution is necessary to understand their nature and properties. Scanning transmission electron microscopy (STEM) combined with electron energy loss spectroscopy (EELS) has become a favourite technique to map LSPR with a nanometer-scale spatial and better than 0.1 eV energy resolution. It utilizes a focused monochromatic electron beam that passes through or near the plasmonic antennas and with a certain (small) probability excites LSPR modes, causing a characteristic energy loss to an electron. The probability of the excitation is experimentally retrieved from energy spectrum of transmitted electrons. It is related to the electric near field component of LSPR parallel with the electron beam E_z and can be used as its representation. Finally, by scanning the electron beam over the plasmonic antenna it is possible to retrieve the spatial distribution of the electric near field of individual LSPR modes.

Babinet's principle, originating in the wave theory of light and diffraction, relates the properties of a planar plasmonic antenna (particle) and a complementary aperture in a thin metal film of the same size and shape. In particular, the energies of LSPR in both antennas shall be identical and the magnetic near-field distribution of the solid antenna shall correspond to the electric near-field distribution of the complementary aperture [2,3]. This link can be readily used to study the magnetic near field in the plasmonic antenna by measuring the electric near field in the complementary aperture.

Results

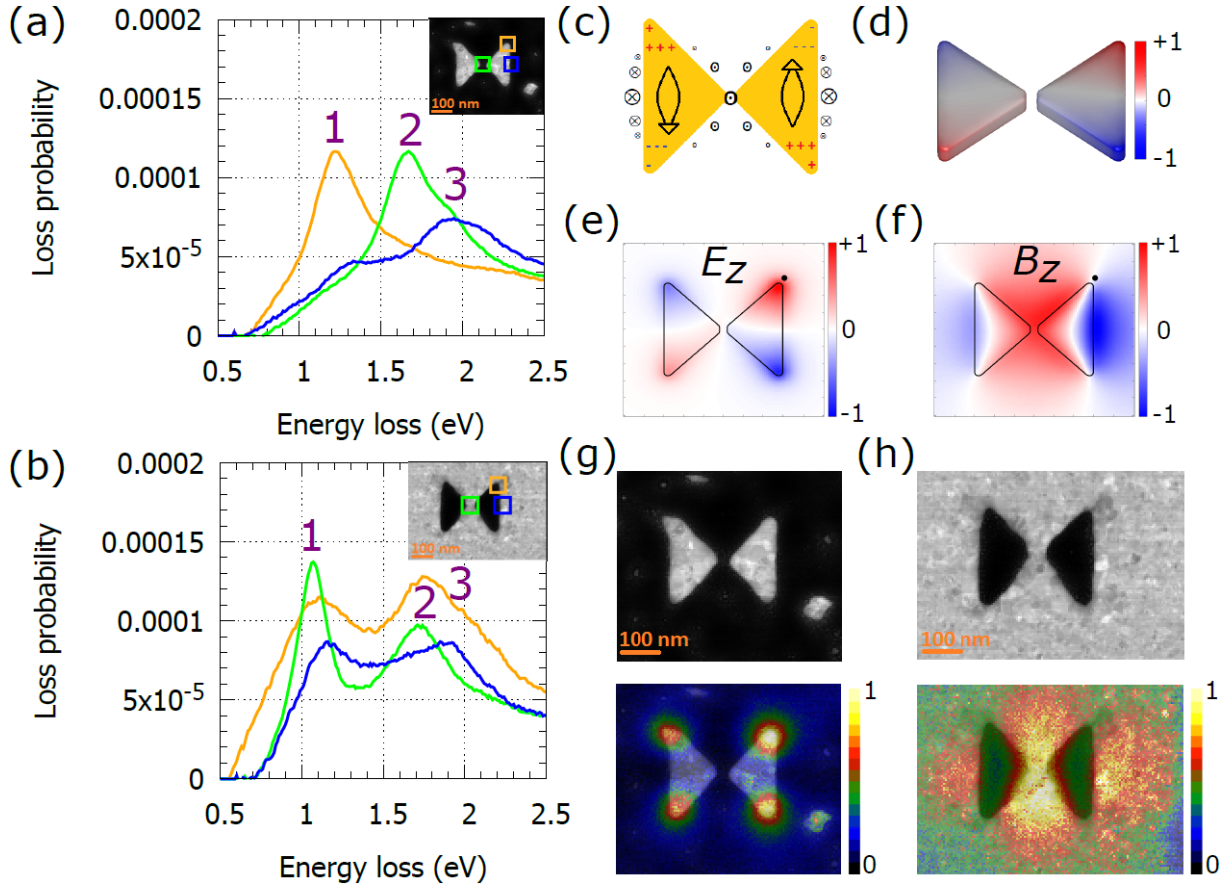

Figure 2: STEM-EELS mapping of the electric and magnetic near field in a bow-tie antenna: EEL spectra featuring three LSPR modes in (a) a bow-tie and (b) an inverted bowtie antenna with a total length of 300 nm. (c) Schematic representation of a transverse dipolar mode with charge oscillations indicated by arrows. (d,e,f) Calculated normalized surface charge distribution (d), electric (e) and magnetic (f) out-of-plane near-field distributions. (g,h) STEM annular dark field micrographs of the bow-tie (g) and inverted bow-tie (h) antenna followed by measured normalized loss probability maps at the energy loss corresponding to the transverse dipolar mode.

We have studied a set of gold bow-tie and diabolo antennas. Such antennas feature areas of extremely concentrated electric or magnetic field, known as hot spots, which are important for a wide range of applications [3]. We demonstrate that combined EELS imaging of a plasmonic antenna and its Babinet-complementary counterpart allows to reconstruct the distribution of both electric and magnetic near fields of LSPR supported by the antenna as well as charge and current antinodes of related charge oscillations [4]. Figure 2(a,b) shows EEL spectra recorded at different positions on a bow-tie (particle) and an inverted bowtie (aperture) antenna with the total length of 300 nm. They reveal three distinct peaks corresponding to three LSPR modes in the antennas. Note that the energy of the three peaks is similar for both structures. In the following, we will consider the lowest-energy peak corresponding to a transverse dipolar LSPR mode. Figure 2(c) shows schematically that charge oscillates along the wings [see arrows in Figure 2(c)] and accumulates at

the corners of the antenna. The loss intensity measured by EELS is related to the plasmon electric field parallel with the trajectory of the electron beam E_z. From Gauss's law, it follows that the strongest out-of-plane electric field E_z occurs just near the areas of the accumulated charge, i.e. near the corners of the bow-tie. Further insight is provided by the calculated induced charge distributions shown in Figure 2(d) and induced electric and magnetic out-of-plane near-field shown in Figure 2(e,f). An experimental loss intensity map for the bowtie at the energy of the first peak in Figure 2(a) is shown in Figure 2(g) and clearly corresponds to the charge distributions shown in Figure 2(d) and the induced electric out-of-plane near-field shown in Figure 2(e). The interpretation of the loss intensity recorded for the inverted bow-tie in Figure 2(h) is less straightforward. It is proportional to the out-of-plane electric field E_z in the inverted bow-tie, which is according to Babinet's principle proportional to the out-of-plane component of the magnetic field B_z in the direct bow-tie. Indeed, magnetic field in the bow-tie according to Ampère's law circulates around the electric current with the maxima around the antinodes of the current as shown in Figure 2(c). Both the experimental loss intensity in the inverted bow-tie [Figure 2(h)] and the calculated out-of-plane magnetic field in the bow-tie [Figure 2(f)] exhibit maxima around the current's antinode inside the gap of the bow-tie and next to the bow-tie's outer edges. In this way, EELS in combination with Babinet's principle can be used for indirect magnetic field imaging [4].

Further, we have studied a set of gold disc-shaped antennas. We have confirmed the qualitative validity of Babinet's principle, but we have found some quantitative differences attributed to the limited theoretical validity of the Babinet's principle: it requires a metal of infinite conductivity and zero thickness, while realistic antennas exhibit finite conductivity and thickness. Interestingly, apertures were found to exhibit stronger plasmonic response than solid antennas, which makes them a remarkable alternative of the usual plasmonic antennas design [2].

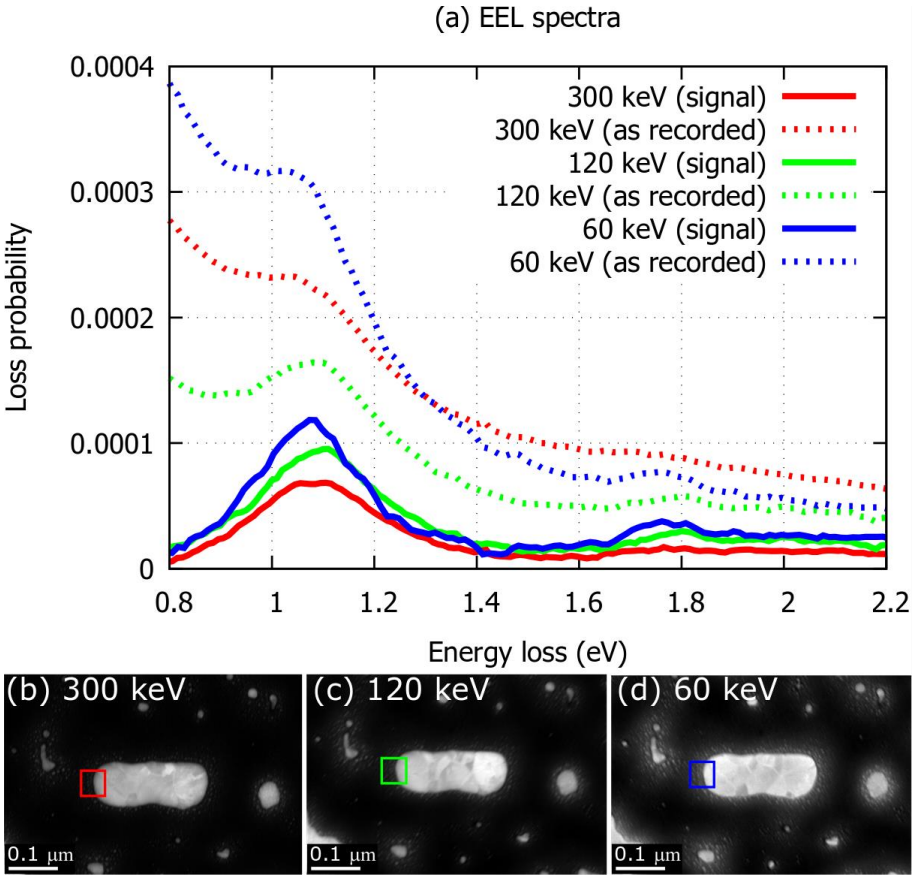

Figure 3: EEL spectra of the same gold rod (240 × 80 × 30 nm^3) at different beam energies: (a) measured raw EEL spectra and extracted signal; (b-d) STEM annular dark field images of the rod with the marked area for integration of EEL spectra in (a) recorded during STEM-EELS mapping at (b) 300 keV, (c) 120 keV, and (d) 60 keV.

We have also studied the influence of the STEM-EELS experimental parameters to the signal-to-background ratio. The ratio improves with the increasing primary beam energy due to suppressed elastic scattering in the sample until the onset of relativistic effects (Čerenkov radiation) which contribute to the background and deteriorate the signal-to-background ratio. I our case, i.e. 30 nm thick gold nanorods on a 30 mn thick SiN_x membrane (Figure 3), the optimal primary beam energy was 120 keV [5].

Conclusion

We have demonstrated the possibility to map the magnetic field by EELS utilizing Babinet's principle. As a proof of concept, we have visualized the magnetic field distribution related to the transverse dipolar plasmonic resonance mode in the bowtie plasmonic antenna. We have indicated quantitative limits of our approach due to limited validity of Babinet's principle. We have also discussed the influence of the EELS parameters to the signal-to-background ratio.

Acknowledgements

Supported by Czech Science Foundation (project No. 17-25799S), European Union's Horizon 2020 program (projects SINNCE, No. 810626, and PETER, No. 737285), MEYS CR (projects CzechNanoLab, No. LM2018110, and CEITEC 2020, No. LQ1601). M. H. acknowledges the support of Thermo Fisher Scientific and CSMS scholarship 2019.

References

[1] Horák M. et al.: *Sci. Rep.* **8** (2018) p. 9640, doi: 10.1038/s41598-018-28037-1.
[2] Horák M. et al.: *Sci. Rep.* **9** (2019) p. 4004, doi: 10.1038/s41598-019-40500-1.
[3] Hrtoň M. et al.: *Phys. Rev. Appl.* **13** (2020) p. 054045, doi: 10.1103/PhysRevApplied.13.054045.
[4] Křápek V. et al.: *Nanophotonics* **9** (2020) p. 623-632, doi: 10.1515/nanoph-2019-0326.
[5] Horák M., Šikola T.: *Ultramicroscopy* (2020), doi: 10.1016/j.ultramic.2020.113044.